

## Self-Organised Droplet Flow Patterns in Microchannels

Pinar OZDEMIR<sup>1</sup>, Stephan MOHR<sup>2</sup>, Changhai WANG<sup>3</sup>, Matthew T. STICKLAND<sup>1</sup>, Nick J. GODDARD<sup>2</sup>,  
Peter R. FIELDEN<sup>2</sup>, Yonghao ZHANG<sup>1,\*</sup>

\* Corresponding author: Tel.: ++44 (0)141 5482854; Fax: ++44 (0)141 5525105; Email: [yonghao.zhang@strath.ac.uk](mailto:yonghao.zhang@strath.ac.uk)  
1: Department of Mechanical Engineering, University of Strathclyde, UK  
2: School of Chemical Engineering and Analytical Sciences, University of Manchester, UK  
3: School of Engineering and Physical Sciences, Heriot-Watt University, UK

**Abstract** In this work, we have investigated the generation and behaviour of self-organised droplet flow patterns in microchannels. The water droplets, which are generated at a T-junction where the carrier is oil, move into an expanded channel and are self reorganised into various flow patterns: single-profile, double-helix-profile, triple-helix-profile, and more. We find that increasing water/oil flow rate ratio and Capillary number lead to more densely packed droplet flow patterns. The channel geometry also plays an essential role where the 300- $\mu\text{m}$ -deep expansion channel can form multiple layers of droplets while only single layer of droplets can be observed in the 200- $\mu\text{m}$ -deep expansion channel.

**Keywords:** Droplet Generation, Micro Channel, Flow Pattern

### 1. Introduction

Chemical/biochemical manipulation of discrete microscopic droplets is a key process in chemical, pharmaceutical and healthcare industries. It is also an important component in microreactors, organic synthesis and polymerase chain reaction for gene analysis and protein crystallisation [1-3]. For example, micro-chemical reactors are excellent for producing low-volume, high-value compounds such as fine chemicals and pharmaceuticals; this technology could therefore revolutionise the nature of chemical engineering and the manufacture of a range of fine chemicals.

The performance of droplet-based microfluidic devices depends on precise control of droplet generation, transportation, coalescence, and interactions with other droplets and surfaces. However, understanding droplet dynamics in microchannels is still in its infancy, which significantly hinders the development of microdroplet technology. In order to obtain new insights in droplet generation and transportation in microchannels, we have investigated non-physically intuitive self-organised droplet flow patterns in expanded flow channels.

Usually, complex flow patterns are formed because

the system is nonlinear and far from equilibrium [4]. Classical examples are Rayleigh-Benard convection and Taylor-Couette oscillatory flow which are caused by flow instability and nonlinearity. However, Thorsen et al. [4] observed unexpected droplet flow patterns in microfluidic channels where the flow is usually laminar and the Navier-Stokes equation becomes linear as the inertial effect is negligible. In this work, we report self-organised water droplet flow patterns within a carrier oil in a confined flow channel experiencing a flow expansion. Furthermore, we have investigated how the flow rate ratio, Capillary number and channel geometry influence the flow patterns.

### 2. Experimental setup

Here, the water droplets are generated in a microfluidic T-junction and the carrier is rapeseed oil. The cross-section of the microfluidic T-junction channel is square with both width and depth of 100  $\mu\text{m}$ . The generated droplets are then moved to an expanded channel of 500  $\mu\text{m}$  of width with depth of 200  $\mu\text{m}$  and 300  $\mu\text{m}$  respectively. The detailed layout of the chip is shown in Figure 1.

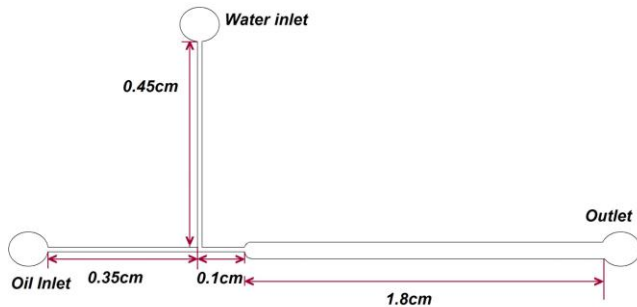


Figure 1. The layout of the microchannels used in the experiments, where both water and oil inlet channels have width and depth of  $100\ \mu\text{m}$ . The width of the expansion channel is  $500\ \mu\text{m}$ , while the depth is  $200$  or  $300\ \mu\text{m}$ .

The inlets of the microfluidic chips are connected to 1 mL syringes via Tygon tubing. Two syringe pumps are used to pump water and rapeseed oil into microchannels with varying flow rate ratio. An optical detection system is used to record the dynamic behavior of droplets. We use a LED light source, Nikon LD Plan Neofluar x20 and x40 objective lens and a CMOS camera (1000 fps) in the optical detection system.

The chips were directly milled on polymethyl methacrylate (PMMA) substrates and sealed with Fisherbrand PCR plate thermal adhesive sealing film. It should be noted that the adhesive sealing film should be carefully placed on the channels to avoid bubble trapping and the bonding becomes stronger after a few hours.

Throughout the experiments, the flow rates have been kept at  $2.7 \times 10^{-5}$  to  $5.55 \times 10^{-4}$  mL/s for the continuous oil phase. The aqueous phase flow rates range from  $1.59 \times 10^{-4}$  to  $3.905 \times 10^{-3}$  mL/s. The water is pumped into the system via a Sage Instruments 355 syringe pump. The advantage of this pump is that it allows the user to increase or decrease the flow rate without stopping the system. Starting with a high flow rate for the aqueous phase can protect the inlet from contamination due to the carrier fluid. When the flow becomes continuous, we are able to decrease the aqueous flow rate, allowing us to collect data in low flow rate regimes as well. The physical properties of the fluids are

given in Table 1.

	Oil	Water
Density (g/mL)	0.9134	0.9983
Viscosity (g/cm s)	0.5196	0.010
Surface tension (g/s <sup>2</sup> )	33.0	73.0

Table 1. Physical properties of the oil (rapeseed oil) and water at the room temperature.

### 3. Results and discussion

When the droplets are generated in a T-shaped junction and move to an expanded channel, the flowfield perturbation due to flow expansion and the resulting pressure loss will cause unstable droplet motion. The droplets will then be self-reorganised to certain stable flow patterns again, which can be seen in figure 2 where the droplets are self-assembled to single-profile, double-helix-profile and triple-helix-profile flow patterns.

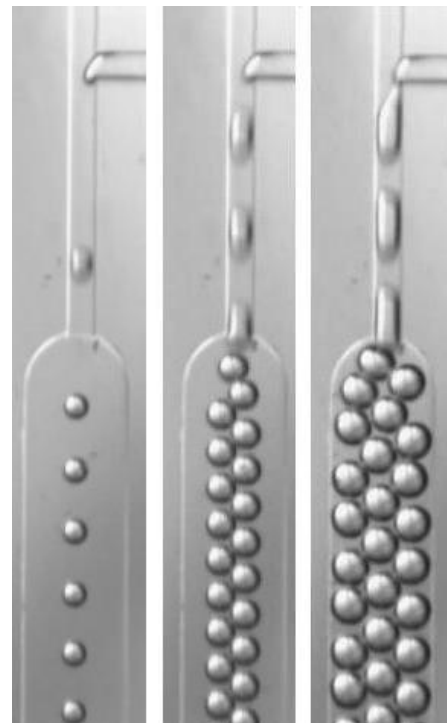


Figure 2. The droplets form different flow patterns when they move into an expansion channel.

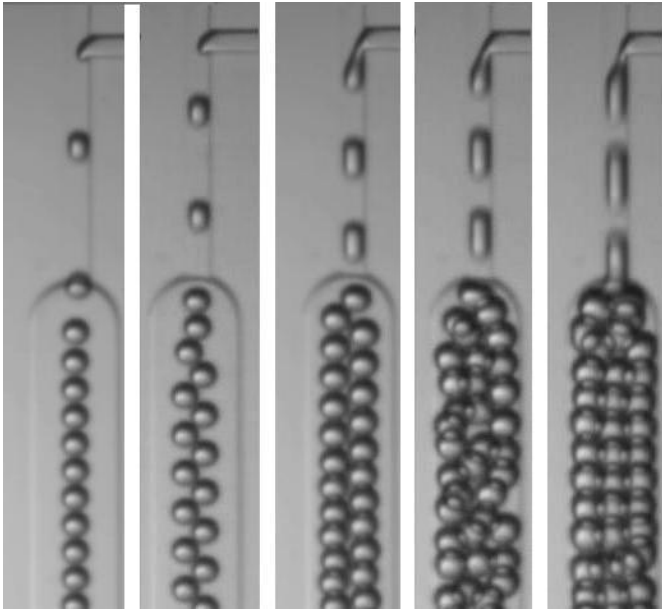


Figure 3. Droplet flow patterns with increasing water/oil flow rate ratio which is 1.14, 2.27, 3.39, 6.23, and 7.38 from left to right. The depth of the expansion channel is 300  $\mu\text{m}$ . The oil flow rate is  $1.39 \times 10^{-4}$  mL/s,  $Re=0.0244$ ,  $Ca=0.02187$ .

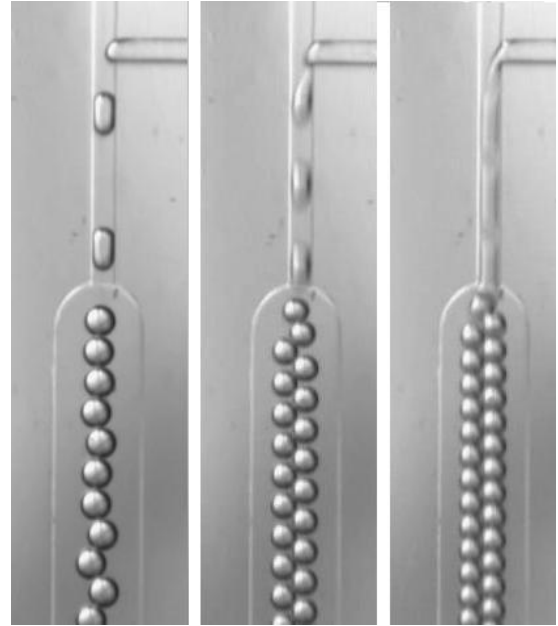


Figure 5. The effect of Capillary number on droplet flow patterns, where  $Ca=0.00875$ ,  $0.00437$ ,  $0.0875$  (from left to right). The water/oil flow rate ratio is fixed at 2.8 while the expansion channel depth is 300  $\mu\text{m}$ .

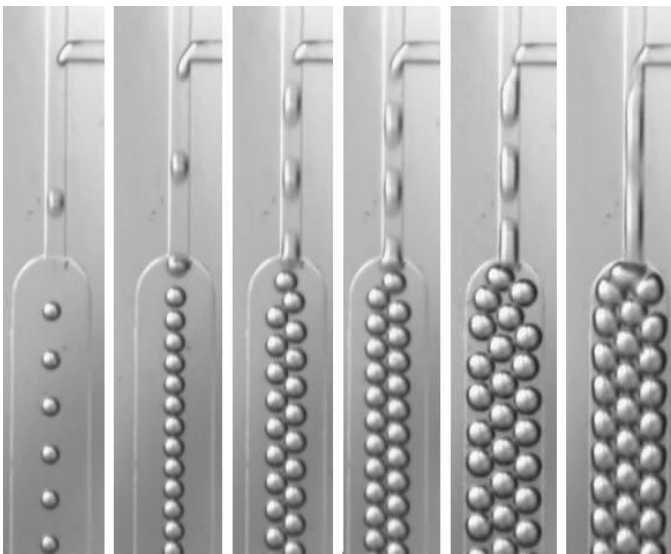


Figure 4. Droplet flow patterns with increasing water/oil flow rate ratio which is 0.57, 1.55, 2.83, 3.97, 5.38 and 14.18 from left to right. The depth of expansion channel is 200  $\mu\text{m}$ . The oil flow rate is  $2.78 \times 10^{-4}$  mL/s,  $Re=0.0488$ ,  $Ca=0.04374$ .

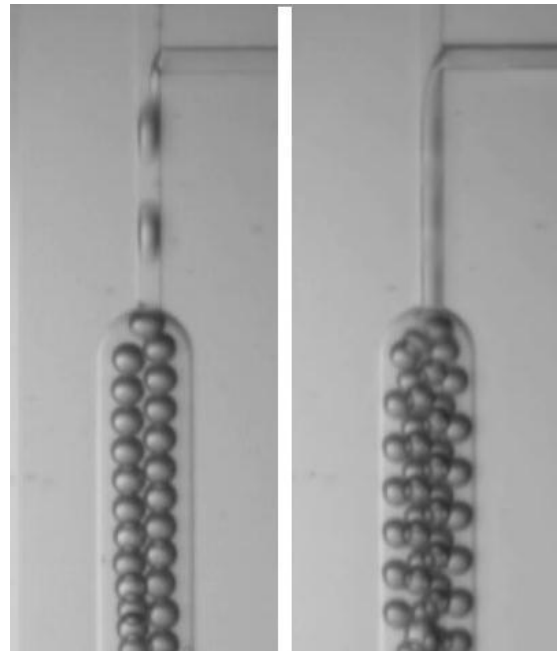


Figure 6. The effect of Capillary number on droplet flow patterns, where  $Ca=0.00437$ ,  $0.0875$  (from left to right). The water/oil flow rate ratio is fixed at 4.3 while the expansion channel depth is 300  $\mu\text{m}$ .

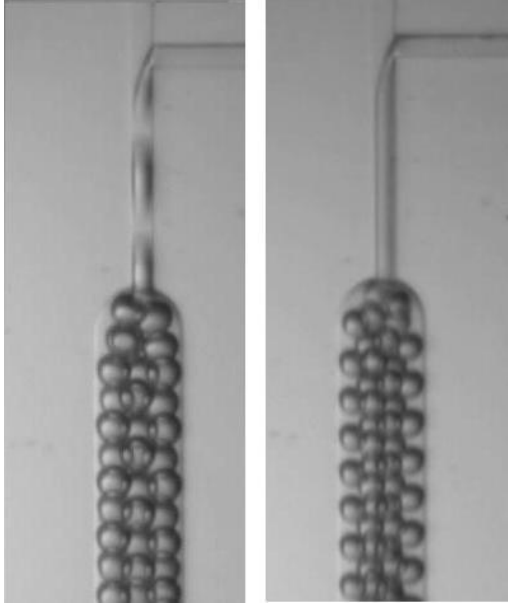


Figure 7. The effect of Capillary number on droplet flow patterns, where  $Ca=0.00437, 0.0875$  (from left to right). The water/oil flow rate ratio is fixed at 7.0 while the expansion channel depth is  $300\ \mu\text{m}$ .

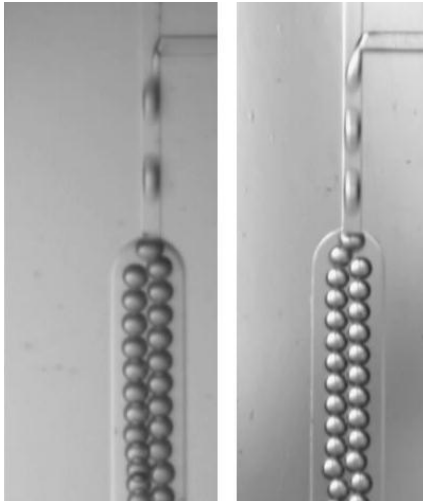
Here, we investigate the underlying physical mechanisms which control those interesting but counter-intuitive phenomena. First, we examine the effect of water/oil flow rate ratio on the droplet self-assembled patterns as shown in figures 3 and 4. In figure 3, the oil flow rate is kept at a constant rate,  $1.39 \times 10^{-4}$  mL/s, while the water/oil flow rate ratio increases from 1.14 to 7.38. The Reynolds number is 0.0244 and the Capillary number is 0.0218. The oil inlet width/depth i.e.  $100\ \mu\text{m}$  and the properties of the oil in Table 1 are used to calculate the Reynolds and Capillary numbers. The depth of the expansion channel is  $300\ \mu\text{m}$  in this experiment. It shows that the transformation of the droplet flow pattern from single-profile to double-helix-profile then to double layer of triple-helix-profile. At the flow rate ratio of 6.23, the flow pattern just transits from an unstable double-helix-profile to a triple-helix-profile. The increasing water/oil flow rate ratio will increase total water droplet volume in the expansion channel once the stable flow patterns are established. Consequently, the droplets have to be packed more densely at a large flow rate ratio, which is confirmed by our observation as shown in

figures 3 and 4. In figure 3 and 4, we also find that increasing water/oil flow rate ratio lead to larger droplets, which is in consistent with the other experimental observations where the droplets are generated in a T-junction [5]. Since the Reynolds number in this work is less than unity, we can ignore the inertial effect and focus on the effect of the Capillary number. When the Capillary number increases from 0.02187 in figure 3 to 0.04374 in figure 4, increasing water/oil flow rate ratio leads to the same phenomenon. Because of the depth of the expansion channel is reduced to  $200\ \mu\text{m}$ , the double layer of the triple helix profile no longer exists due to the restriction of the geometry. The effect of the channel geometry will be examined later.

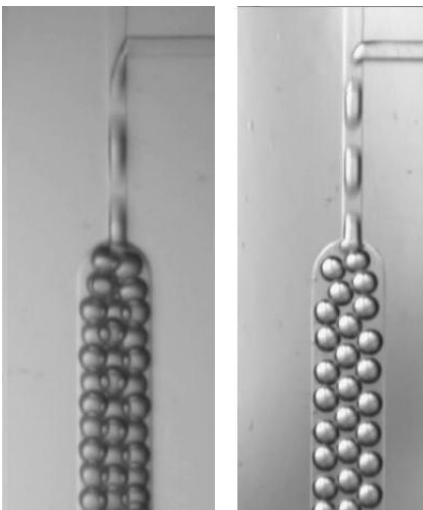
Secondly, we investigate the effect of the Capillary number on droplet pattern formation. Figure 5 shows the droplet flow patterns are significantly different at different Capillary numbers while the other operating conditions are kept the same including the flow rate ratio. Since the larger the Capillary number, the smaller the droplets will be [5], more droplets are generated in a certain period of time. More densely packed droplets are therefore formed as the Capillary number increases, which is confirmed by the flow patterns in figures 5-7. As the water/oil flow rate ratio also increases from 2.8 to 7.0, which leads to smaller droplets, the number of the generated droplets increases. Consequently, the droplets are more densely organised as shown in figure 7.

Finally, we examine the geometry effect by comparing droplet flow patterns at two different depths of expansion channels i.e.  $200\ \mu\text{m}$  and  $300\ \mu\text{m}$  respectively. By comparing the left and right columns in both figures 8 (a-c) and 9 (a-c), we can find the droplets are more densely packed for the deep expansion channel i.e. the one with  $300\ \mu\text{m}$  of depth. Because the water/oil flow rate ratio and capillary number are the same for the corresponding left and right column figures, the generated droplet size at T-junction is approximately the same. In addition to the more rapid drop of the flow rate, the deeper expansion channel has room in the depth direction to allow the droplets to self-organise in

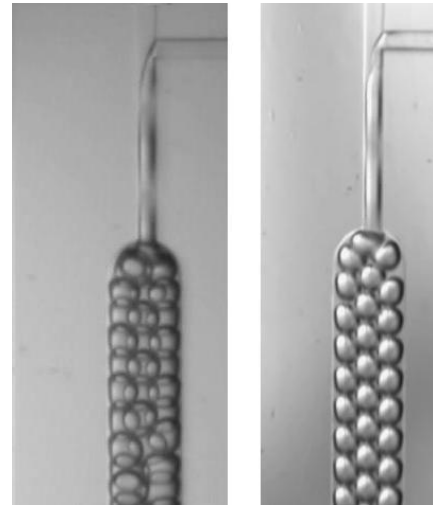
that direction. Therefore, the droplet flow patterns are 3-dimensional in the 300- $\mu\text{m}$ -deep expansion channel while they are 2-dimensional in the 200- $\mu\text{m}$ -deep expansion channel. Consequently, the number of droplets can stay in the expansion channel at any given time can be more in the 300- $\mu\text{m}$ -deep expansion channel, despite the water/oil flow rate ratios are the same.



(a)



(b)



(c)

Figure 8. The effect of expansion channel depth on the droplet flow patterns where  $Re = 0.049$ ,  $Ca=0.0437$  and the depths are 300  $\mu\text{m}$  (the left column) and 200  $\mu\text{m}$  (the right column) respectively. The water/oil flow rate ratio is (a) 4.25; (b) 47.1; and (c) 14.1.

#### 4. Conclusion

A series of experiments have been performed to examine the droplet generation and flow patterns in microchannels where the Reynolds number is less than unity. Generally, we find that the droplet size decreases when the Capillary number increases. Large Capillary number and water/oil flow rate ratio will lead to more densely organised droplet flow patterns. We also find that the channel geometry plays an important role as well.

Although this preliminary study reveals interesting self-organised droplet flow patterns and the underlying physical mechanisms, more quantitative study is currently underway to provide more precise data such as droplet size in order to understand droplet dynamics in microchannels.

## References

- [1] B. T. Kelly, J. C. Baret, V. Taly, A. D. Griffiths, (2007) *Chem. Commun.* 18: 1773.
- [2] S. Mohr, Y. H. Zhang, A. Macaskill, P. J. R. Day, R. W. Barber, N. J. Goddard, D. R. Emerson, P. R. Fielden, (2007) *Microfluidic Nanofluidic* 3: 611.
- [3] S.-Y. Teh, R. Lin, L.-H. Hung, A. P. Lee, (2008) *Lab Chip* 8: 198.
- [4] T. Thorsen, R. W. Roberts, F. H. Arnold, S. R. Quake, (2001) *Phys. Rev. Lett.* 86: 4163.
- [5] P. Garstecki, M. J. Fuerstman, H. A. Stone, G. M. Whitesides, (2006) *Lab Chip* 6: 437.

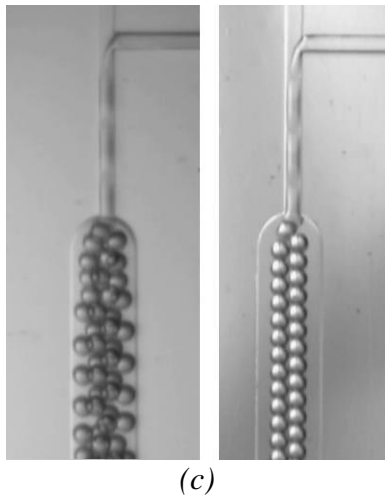
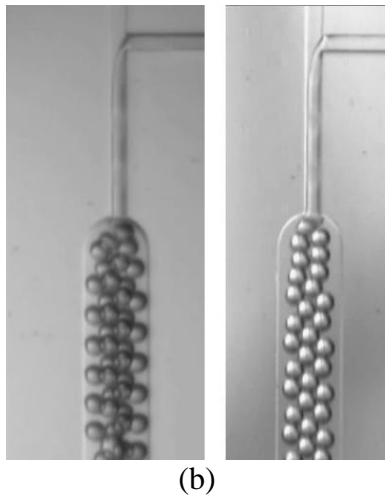
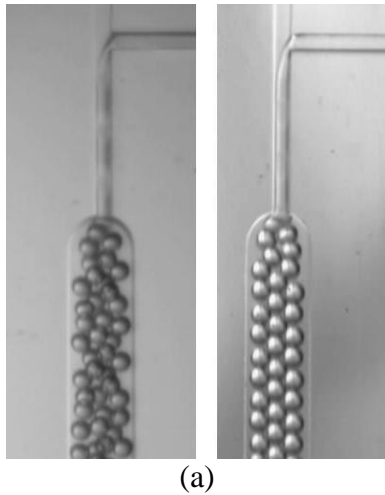


Figure 9. The effect of expansion channel depth on the droplet flow patterns ( $Re=0.098$ ,  $Ca=0.0875$ ) where the depth is  $300\ \mu\text{m}$  (the left column) and  $200\ \mu\text{m}$  (the right column). The water/oil flow rate ratio is (a) 3.5; (b) 4.25; and (c) 5.0.